PERGAMON

International Journal of Solids and Structures 36 (1999) 5331–5355

INTERNATIONAL JOURNAL OF SOLIDS and STRUCTURES

www.elsevier.com/locate/ijsolstr

Anisotropic yield criterion for polycrystalline metals using texture and crystal symmetries

A.M. Maniatty*, J.-S. Yu[1], T. Keane

Department of Mechanical Engineering, Aeronautical Engineering and Mechanics, Rensselaer Polytechnic Institute, 110 8th Street, Troy, NY 12180-3590, U.S.A.

Received 30 May 1996; in revised form 29 July 1998; accepted 10 August 1998

Abstract

An anisotropic yield criterion for polycrystalline metals which uses texture data and takes advantage of crystal symmetries is presented. A linear transformation is developed to map an anisotropic yield surface for a polycrystal to an appropriate isotropic yield surface. The transformation developed reflects the symmetry of the material being modeled. First, the transformation is determined. Then, information regarding the orientation distribution (texture) of the crystals in a polycrystalline aggregate is used to determine, via averaging, the transformation for the polycrystal. The transformation, along with appropriate isotropic yield surface, provides a phenomenological approach to modeling yield, yet accounts for microstructural texture. The approach reduces to the Hill (1950) anisotropic plasticity theory under certain conditions. The yield surfaces and *R*-values for various face-centered-cubic (fcc) polycrystalline textures are computed by this method. Results compare favorably with those given by other theories, and with experiment. The method proves to have the computational efficiency of phenomenological approaches to modeling yield, while effectively incorporating the physics of more complex crystallographic approaches.

1. Introduction

There are generally two approaches for determining yield surfaces in polycrystalline metals: the continuum approach and the crystallographic approach. The continuum approach has the advantage of being relatively simple, with yield surfaces defined in a functional form in terms of stress and resistance to plastic flow. The drawback of the continuum approach is that continuum yield functions are often unable to capture the shape of a yield surface accurately. These yield functions generally do not account for material microstructure, particularly microstructural

* Corresponding author. Fax: 518 276 6025; e-mail: maniaa@rpi.edu

[1] Currently at Institute of Nuclear Energy Research, Lung-Tam, Taiwan, Republic of China.

0020-7683/99/$ - see front matter
PII: S0020-7683(98)00248-0

texture, which can affect surface shape significantly. Yet in many applications, it is important to accurately account for yield surface shape, for example when modeling sheet forming and calculating forming limits (see for example Lian et al., 1989). An alternative to the continuum approach is the crystallographic approach, which does attempt to account for the physics underlying yield surface shape by defining metal yielding behavior in terms of the microstructural phenomenon of crystallographic slip. The crystallographic method is better able to predict shapes of yield surfaces, but is a much more complex approach, requiring time-consuming computations to map out the yield surface. The work presented herein is an attempt to bridge these two approaches (continuum and crystallographic) by exploiting the symmetries found in each grain of a polycrystalline metal, and by making use of the isotropic plasticity equivalent (IPE) method of Karafillis and Boyce (1993). Because there are a large number of continuum yield models and crystallographic yield models, it is necessary to discuss those models that will form the basis of the present approach.

In the continuum approach, a phenomenological yield criterion, which is a function of the stress, is used to define the yield surface in stress space. For isotropic material behavior the Tresca and von Mises yield criteria are the most widely used. Hosford (1972) connected the Tresca and von Mises criteria by proposing a generalized isotropic yield criterion which has the Tresca and von Mises yield criteria as lower and upper bounds, respectively. Karafillis and Boyce (1993) extended Hosford's criterion by incorporating a new upper bound. Anisotropic continuum yield criteria have also been proposed. Hill (1950) developed a quadratic yield function for orthotropic materials and later Barlat et al. (1991) developed a non-quadratic yield function for orthotropic materials. Karafillis and Boyce (1993) introduced an anisotropic yield criterion formulated using the IPE concept. The criterion is an extension of their generalized isotropic yield criterion. The method they presented uses a linear mapping to model the connection between an anisotropic yield surface and their previously-mentioned generalized isotropic yield surface. The linear mapping can reflect the symmetries of the anisotropic material. In the present work, the IPE continuum approach to anisotropic plasticity is connected to a crystallographic approach.

In crystallographic approaches to yield surface modeling, the yield surface of a polycrystalline aggregate is determined from the yielding behavior of each grain in the aggregate. For moderately textured polycrystals, it is assumed that each grain has the same critical resolved shear stress on each of its slip systems (Taylor and Elam, 1925). Thus each grain has the same yield surface, and differs from the others only in its orientation. The yield surface in each grain is determined from the yielding behavior of the grain's crystallographic slip systems. Bishop and Hill (1951a, b), using the principle of maximum work, outlined a procedure for calculating the yield stresses of polycrystalline aggregates given data about individual grain slip systems. They used Taylor's (1938) assumption for the interaction law, i.e. they assumed that each grain undergoes the same homogeneous deformation as the macroscopic deformation. In their calculation, Bishop and Hill assumed a random texture, so the result calculated described yielding of an isotropic polycrystalline aggregate. Following the same procedure, Viana et al. (1979) used different textures to find the isotropic and anisotropic yield surfaces in sheet metals in the (T_{11}–T_{22}) stress plane under plane stress loading conditions (**T** being the stress tensor). Including the shear stress, T_{12}, Barlat and Richmond (1987) use the same approach to calculate the tricomponent yield surface for several textures that are commonly observed after the deformation or recrystallization processes. Barlat et al. (1997) have shown that the Bishop and Hill (1951a, b) yield surfaces correspond well with

experimentally determined yield surfaces for a number of anisotropic polycrystalline textures, providing justification for the application of Taylor and Elam's (1925) hardening hypothesis and Taylor's (1938) interaction law to textured polycrystals. Bishop and Hill (1951a) showed by comparison to experiments that the application of Taylor's hypothesis to isotropic polycrystals is justifiable.

In the present work, with the aid of the IPE method proposed by Karafillis and Boyce (1993), a continuum yield function is developed for fcc polycrystalline metals. The goal is to formulate a criterion that is not only computationally efficient, but that also can account for microstructural texture in modeling the yield surface. In order to bring microstructural information into the continuum model, both of the Taylor assumptions mentioned above are used. While the assumptions do provide for good agreement with experiments (Barlat et al., 1997), the present work limits their application to modeling weakly-textured materials (50% random in all cases). This avoids the theoretical difficulties that arise in the application of the hypotheses to polycrystals in which grains may have pronounced heterogeneity in slip-system hardness and morphology. To further limit the reliance on the Taylor (1938) interaction law, it is applied only to the plastic part of polycrystalline deformation, and only small to moderate deformations to the textured polycrystal are considered. The assumptions and limitations are used as a first step in the expected development of a more sophisticated continuum model that more completely accounts for microstructural features. Precise modeling of crystallographic behavior, as in the Bishop and Hill (1951a, b) model or subsequent self-consistent models by Hill (1965) and Harren (1991) would sacrifice the computational efficiency that is a central goal of the present work.

To develop the continuum yield function, it is first noted that if each slip system in a grain has the same critical resolved shear stress, it is expected that the yield criterion for each grain will reflect the natural symmetries of the grain's lattice. Crystallographic yield formulations have not exploited these symmetries as much as possible. The subsequent development includes the appropriate crystal symmetries in the IPE formulation. The crystallographic yield theory of Bishop and Hill (1951a, b) is used to determine the parameters for the IPE linear transformation tensor for a single fcc crystal. Then, by using Taylor's (1938) theory for grain interaction, and by assuming that rates of work in the anisotropic and IPE materials are equal, it is possible to find the IPE transformation tensor for a polycrystal, using only polycrystalline texture data. The yield predictions given by this method are compared to the results presented in Barlat and Richmond (1987), which were computed using a crystallographic approach. The criterion is also compared with the Hill (1950) continuum criterion, and is shown to be a generalization of that criterion. Finally, the R-values predicted by the new IPE method are investigated through comparison with experimental data, since in the past, purely crystallographic approaches have generally not predicted R-values well (Karafillis and Boyce, 1993).

2. Isotropic plasticity equivalent (IPE) method

The IPE method presented by Karafillis and Boyce (1993) assumes that there exists a fourth-order linear transformation tensor, $\boldsymbol{L}$ which transforms the actual second-order stress tensor, $\mathbf{T}$, acting on an anisotropic material into a new second-order stress tensor, $\mathbf{S}$, acting on an 'isotropic plasticity equivalent' material. The tensor $\mathbf{S}$ is called the 'isotropic plasticity equivalent' stress

tensor. The new stress tensor **S** is used in an isotropic yield criterion which in effect models the transformed yield surface of the original anisotropic material. In order to model an anisotropic yield surface by this method, it is necessary to find both the transformation tensor $\boldsymbol{L}$ and the isotropic yield function that together allow for an accurate representation of a material's anisotropic behavior.

Henceforth, quantities that refer to the actual anisotropic material will be said to lie in the 'physical' domain; quantities that arise from application of the IPE transformation $\boldsymbol{L}$ will be said to lie in the 'IPE' domain, and will be said to act on the 'IPE' material.

2.1. Single crystals

In the following development, cubic crystals, specifically face-centered cubic (fcc) crystals, are considered. Since both the actual stress **T** on the anisotropic material and the IPE stress **S** on the 'equivalent' isotropic material are symmetric second-order tensors, both may be represented as vectors, according to the usual tensor contraction methods outlined by Nye (1957). Thus,

$$\mathbf{T} = \{T_{11}, T_{22}, T_{33}, 2T_{32}, 2T_{31}, 2T_{21}\} \tag{1a}$$

$$\mathbf{S} = \{S_{11}, S_{22}, S_{33}, S_{32}, S_{31}, S_{21}\}. \tag{1b}$$

Similarly, assuming the fourth-order transformation tensor $\boldsymbol{L}$ possesses both major and minor symmetries $L_{ijkl} = L_{jikl} = L_{ijlk} = L_{klij}$, it may be contracted to a 6×6 matrix that operates on the vector form of **T** according to the rules of linear algebra. In tensor notation

$$\mathbf{S} = \boldsymbol{L}[\mathbf{T}] \tag{2}$$

where, following Gurtin (1981), brackets ([]) indicate the operation of a fourth-order tensor on a second-order tensor. If the components of the physical stress tensor **T** are with respect to the lattice coordinates, in order to maintain cubic symmetry, the matrix of components of $\boldsymbol{L}$ must have the form

$$[\boldsymbol{L}] = \begin{bmatrix} a & c & c & 0 & 0 & 0 \\ c & a & c & 0 & 0 & 0 \\ c & c & a & 0 & 0 & 0 \\ 0 & 0 & 0 & \frac{1}{2}b & 0 & 0 \\ 0 & 0 & 0 & 0 & \frac{1}{2}b & 0 \\ 0 & 0 & 0 & 0 & 0 & \frac{1}{2}b \end{bmatrix}, \tag{3}$$

where a, b and c are constants. The components of (3) that transform the shear stresses are chosen to be $\frac{1}{2}b$ in order to simplify algebra in subsequent analyses.

As will be shown later, if the yielding behavior is assumed to be independent of the mean stress, then the constants a and c will be linearly related. It is then possible to select c arbitrarily, and then determine a uniquely. So, c can be set equal to zero without altering the results. Setting c equal to zero reduces the matrix $\boldsymbol{L}$ given in (3) to a diagonal matrix, when expressed with respect to the lattice coordinates of the crystal. A diagonal matrix $\boldsymbol{L}$ can be considered an affine

transformation which 'stretches' the yield surface along the axes of the six-dimensional stress space (in coordinate system of the crystal).

In addition to a definition of the transformation tensor $\boldsymbol{L}$, the IPE formulation requires the selection of an isotropic yield criterion to govern the yielding behavior of the transformed IPE stress. The isotropic yield criterion used herein is the one proposed by Hosford (1972). It has the form

$$|s_1 - s_2|^m + |s_2 - s_3|^m + |s_3 - s_1|^m = 2Y^m \tag{4}$$

where s_1, s_2, and s_3 are the principal stresses of the IPE stress tensor $\mathbf{S}$, Y is an arbitrarily-chosen uniaxial yield stress for the IPE material, and m is a material constant. It should be noted that this yield criterion reduces to the von Mises yield criterion for $m = 2$ and to the Tresca criterion for $m \to \infty$. In addition, this yield criterion predicts yielding that is independent of the mean stress.

To calibrate the IPE criterion, it is necessary to determine the optimal parameters a and b that fit the physical anisotropic yield surface to the isotropic yield surface defined by (4). The anisotropic yield surface to be transformed is the crystallographic yield surface for an fcc single crystal derived by Bishop and Hill (1951a, b). Bishop and Hill (1951a, b) showed that the slip-plane-based yield surface of an fcc crystal is composed of 24 planes with 56 vertices in five-dimensional deviatoric stress space. These results are based on a rate-independent theory which postulates that yielding occurs on a slip system when the resolved shear stress on that slip system reaches a critical value—the critical resolved shear stress. To calibrate the IPE model to the Bishop and Hill (1951a, b) crystallographic surface, the IPE criterion will be fit to the crystallographic surface at the midpoints of the 24 planes and at the 56 vertices. Kocks et al. (1983) have tabulated the yielding stress states that correspond to the 56 vertices. Transforming each of these stress states with the linear transformation tensor $\boldsymbol{L}$ given in eqn (3) and then computing the principal stresses of the resulting IPE stress tensors, the following five categories of principal IPE stresses result. (The number of vertices that fall into each category is also listed.)

1. $\langle \frac{2}{3}(a-c)\tau, -\frac{1}{3}(a-c)\tau, -\frac{1}{3}(a-c)\tau \rangle$, (6 vertices)
2. $\langle b\tau, -\frac{1}{2}b\tau, -\frac{1}{2}b\tau \rangle$, (8 vertices)
3. $\langle 0, b\tau, -b\tau \rangle$, (6 vertices)
4. $\langle -\frac{1}{6}(a-c)\tau, \frac{1}{12}(a-c)\tau + \tau\sqrt{\frac{1}{16}(a-c)^2 + \frac{1}{2}b^2}, \frac{1}{12}(a-c)\tau - \tau\sqrt{\frac{1}{16}(a-c)^2 + \frac{1}{2}b^2} \rangle$, (24 vertices)
5. $\langle 0, +\frac{1}{2}\tau\sqrt{(a-c)^2 + b^2}, -\frac{1}{2}\tau\sqrt{(a-c)^2 + b^2} \rangle$, (12 vertices).

In the above equations, $\tau = \sqrt{6}\tau_c$ and τ_c is the critical resolved shear stress for each of the twelve primary slip systems. Following the same procedure, the IPE stresses are computed for each of the 24 planes on the crystallographic yield surface at the midpoints of these planes. The midpoints of the planes are found by averaging the locations of the vertices bounding each of the planes. The principal stresses of the IPE stress tensors at the midpoints of each of these planes are the same, namely:

6. $\langle 0, +\frac{1}{32}\tau\sqrt{49(a-c)^2 + 162b^2}, -\frac{1}{32}\tau\sqrt{49(a-c)^2 + 162b^2} \rangle$, (24 vertices).

The above equations demonstrate that only the value of $(a-c)$ is important, and the individual values of a and c have no influence on the yield behavior, as mentioned earlier.

For each set of principal stresses, a residual function f_i, $i = 1, \ldots, 6$, can be defined by substituting the principal stresses into eqn (4) and rearranging it as

$$f_i = |s_{1_i} - s_{2_i}|^m + |s_{2_i} - s_{3_i}|^m + |s_{3_i} - s_{1_i}|^m - 2Y^m, \tag{5}$$

where f_1, f_2, f_3, f_4 and f_5 are residuals defined for the five categories of vertices, and f_6 is the residual function at the midpoints of the planes. An objective function F can be defined as

$$F = 6f_1^2 + 8f_2^2 + 6f_3^2 + 24f_4^2 + 12f_5^2 + 24f_6^2 + (6f_1 + 8f_2 + 6f_3 + 24f_4 + 12f_5 + 24f_6)^2. \tag{6}$$

By minimizing the objective function F, the optimal values of $(a-c)$ and b (or just a and b if $c = 0$) can be determined. The objective function given by eqn (6) was constructed to allow the transformed Bishop and Hill (1951a, b) yield surface features listed above to simultaneously satisfy the yield criterion given by eqn (4). The first six terms in the objective function are the residuals for each of the six classes of yield surface features, weighted by the number of occurrences of each feature. Each of these first six terms is squared, in order to avoid non-zero positive and negative residuals cancelling each other. The last term in the objective function (in parentheses) stabilizes the numerics of the minimization for high values of the exponent m. In the numerical procedure, each of the residuals is normalized by the effective Hosford (1972) yield stress Y (chosen by the analyst) leading to residuals from the first six terms that become small enough to exceed machine precision before convergence, when m is large. The last term provides the procedure with values within machine precision with which to complete the minimization.

With $c = 0$, the optimal values of a and b given by the objective function are listed in Table 1 for different exponents m. Projections of the IPE fit to the Bishop and Hill (1951a, b) yield surface

Table 1
Optimal values of a and b and normalized residual values $\sqrt[m]{F}/\tau_c$ corresponding to different values of m

m	a	b	$\sqrt[m]{F}/\tau_c$
2	1.42052	0.90279	7.00014
4	1.37925	0.86712	3.32431
6	1.33901	0.81945	2.43548
8	1.31104	0.78156	2.05834
10	1.28730	0.75359	1.84107
12	1.26576	0.73337	1.69632
14	1.24644	0.71861	1.59239
16	1.22948	0.70753	1.51414
18	1.21484	0.69891	1.45319
20	1.20230	0.69197	1.40445

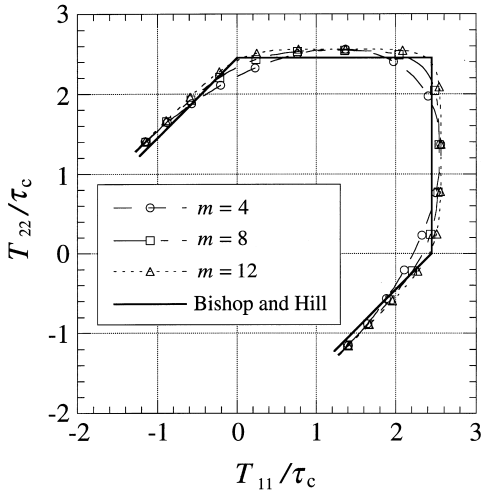

Fig. 1. Bishop and Hill yield surface for a single fcc crystal and approximated surfaces calculated with the IPE method using different values of m on normalized T_{11}–T_{22} plane.

for $m = 4$, 8 and 12 are shown in Fig. 1, along with a projection of the Bishop and Hill (1951) yield surface itself. Notice in Table 1 and Fig. 1 that the IPE surface approximation to the Bishop and Hill (1951a, b) yield surface is better for larger values of m, since the corners in the surface can be better approximated.

2.2. Relation between IPE and Hill (1950) criteria

The IPE approach for modeling anisotropy can be viewed as a generalization of the continuum approach developed by Hill (1950). Hill proposed modeling yield in anisotropic materials with a function similar to the Mises yield function, but with modifications to account for material anisotropies up to orthotropic. Hill's function predicts yielding that is independent of hydrostatic stress:

$$f^{\text{Hill}} = \alpha_{12}(T_{11}-T_{22})^2+\alpha_{23}(T_{22}-T_{33})^2+\alpha_{31}(T_{33}-T_{11})^2 + 6\alpha_{44}T_{12}^2+6\alpha_{55}T_{23}^2+6\alpha_{66}T_{13}^2-2Y^2. \quad (7)$$

The Y term in eqn (7) is an arbitrarily chosen 'equivalent' yield stress for the material, and the coefficients α are determined from a series of six yield tests by the relations

$$\alpha_{12} = Y^2\left(\frac{1}{P^2}+\frac{1}{Q^2}-\frac{1}{R^2}\right) \quad \alpha_{44} = \frac{1}{3}Y^2\left(\frac{1}{V^2}\right)$$

$$\alpha_{31} = Y^2\left(\frac{1}{R^2}+\frac{1}{P^2}-\frac{1}{Q^2}\right) \quad \alpha_{55} = \frac{1}{3}Y^2\left(\frac{1}{T^2}\right)$$

$$\alpha_{23} = Y^2\left(\frac{1}{Q^2}+\frac{1}{R^2}-\frac{1}{P^2}\right) \quad \alpha_{66} = \frac{1}{3}Y^2\left(\frac{1}{U^2}\right) \tag{8}$$

where P, Q, R are the yield stresses in uniaxial tension with respect to the principal axes of anisotropy, and T, U, V are the corresponding yield stresses in shear.

The IPE criterion, which consists of both the transformation tensor $\boldsymbol{L}$ and the Hosford (1972) yield function, reduces to the Hill criterion when $m = 2$, $\boldsymbol{L}$ has orthotropic symmetry and $\boldsymbol{L}$ has the additional constraint that deviatoric tensors are transformed to the deviatoric tensors, i.e.,

$$\mathbf{S}' = \boldsymbol{L}[\mathbf{T}'], \tag{9}$$

where prime ($'$) denotes the deviatoric part of the tensor. This condition is necessary when yielding in the physical domain is taken to be independent of the hydrostatic stress, as it is in the Hill (1950) criterion. [Yielding in the IPE domain is always independent of the hydrostatic stress by Hosford's (1972) yield criterion, eqn (4).] To explicitly specify the constraints on $\boldsymbol{L}$, note that $\mathbf{S}'$ and $\mathbf{T}'$ are defined as

$$\mathbf{S}' = \mathbf{S} - \tfrac{1}{3}\mathrm{tr}(\mathbf{S})\boldsymbol{I} = \boldsymbol{L}[\mathbf{T}] - \tfrac{1}{3}\mathrm{tr}(\boldsymbol{L}[\mathbf{T}])\boldsymbol{I}, \tag{10a}$$

$$\mathbf{T}' = \mathbf{T} - \tfrac{1}{3}\mathrm{tr}(\mathbf{T})\boldsymbol{I}, \tag{10b}$$

where $\boldsymbol{I}$ is the second-order identity tensor and tr( ) is the trace operator. Substituting eqns (10) into (9), the condition for pressure-independent yield in the physical domain can be simplified to

$$\mathrm{tr}(\boldsymbol{L}[\mathbf{T}])\boldsymbol{I} = \mathrm{tr}(\mathbf{T})\boldsymbol{L}[\boldsymbol{I}], \tag{11a}$$

or, in indicial notation

$$L_{ijkl}T_{kl}\delta_{ij}\delta_{mn} - L_{mntu}T_{pq}\delta_{pq}\delta_{tu} = 0, \tag{11b}$$

where δ_{ij} is the Kronecker delta. Factoring and simplifying eqn (11b), the constraints on the IPE transformation $\boldsymbol{L}$ that produce deviatoric yield are found to be

$$(L_{1111}-L_{2222}) = (L_{2233}-L_{1133}), \quad L_{1132}+L_{2232}+L_{3332} = 0, \tag{12a,b}$$

$$(L_{2222}-L_{3333}) = (L_{1133}-L_{1122}), \quad L_{1131}+L_{2231}+L_{3331} = 0, \tag{12c,d}$$

$$(L_{3333}-L_{1111}) = (L_{1122}-L_{2233}), \quad L_{1121}+L_{2221}+L_{3321} = 0. \tag{12e,f}$$

As long as these constraints are met, yielding in the physical domain will be independent of the hydrostatic stress.

Consider the transformation tensor $\boldsymbol{L}$ for a crystal with cubic symmetries, given by eqn (3). The components of this tensor identically satisfy eqns (12), so for a cubic crystal, the IPE criterion can readily reduce to the Hill criterion. Using the form of $\boldsymbol{L}$ given in (3), the physical stress $\mathbf{T}$ can be transformed to the IPE stress $\mathbf{S}$, which can in turn be substituted into the Hosford (1972) $m = 2$ function to produce a form of the IPE yield function for a material with cubic symmetry:

$$f^{\mathrm{IPE}} = (a-c)^2(T_{11}-T_{22})^2 + (a-c)^2(T_{22}-T_{33})^2 + (a-c)^2(T_{33}-T_{11})^2 + 6b^2T_{12}^2 + 6b^2T_{23}^2 + 6b^2T_{13}^2 - 2Y^2. \tag{13}$$

Equation (13) is identical to the Hill (1950) criterion for a cubic crystal, with $\alpha_{12} = \alpha_{23} = \alpha_{31} = (a-c)^2$, and $\alpha_{44} = \alpha_{55} = \alpha_{66} = b^2$. Note that the IPE equivalent yield stress—which is chosen arbitrarily—has been chosen to be identical to the Hill equivalent yield stress of eqn (7). Also note that, as discussed earlier, only one of the components a and c is independent.

For an orthotropic material, the IPE transformation tensor displays orthotropic symmetries:

$$\boldsymbol{L} = \begin{bmatrix} a & b & c & 0 & 0 & 0 \\ b & d & e & 0 & 0 & 0 \\ c & e & f & 0 & 0 & 0 \\ 0 & 0 & 0 & \frac{1}{2}g & 0 & 0 \\ 0 & 0 & 0 & 0 & \frac{1}{2}h & 0 \\ 0 & 0 & 0 & 0 & 0 & \frac{1}{2}j \end{bmatrix}. \tag{14}$$

Performing the same procedure using this form of $\boldsymbol{L}$, the relationship between the Hill (1950) and IPE parameters is found to be:

$$\begin{aligned} \alpha_{12} &= (a^2 + c^2 + f^2 - fa) + ad - 2ca + 4fc + 4d^2 - 4dc - 5df, \\ \alpha_{23} &= (a^2 + c^2 + f^2 - fa) - 5ad + 4ca - 2fc + 4d^2 - 4dc + df, \\ \alpha_{13} &= (a^2 + c^2 + f^2 - fa) + ad - 2ca - 2fc - 2d^2 + 2dc + df, \\ \alpha_{44} &= j^2, \\ \alpha_{55} &= g^2, \\ \alpha_{66} &= h^2, \end{aligned} \tag{15a}$$

with the following constraints between IPE parameters:

$$\begin{aligned} (a-d) &= (e-c), \\ (d-f) &= (c-b). \end{aligned} \tag{15b}$$

The constraints in eqn (15b) correspond to eqns (12a) and (12c), respectively. A third constraint on the IPE parameters is implicit in (15a), namely that a, c, and f are not independent. Note that the application of the constraints (12) allow the more general IPE criterion (with nine parameters) to uniquely map to the Hill (1950) criterion (with six parameters to describe materials of the same symmetry).

The IPE criterion is more general than the Hill (1950) criterion, in that it can model material anisotropies greater than orthotropic and in that it may take forms that are non-quadratic (by selecting the exponent $m \neq 2$). Examining eqns (13) and (15), it is also apparent that the IPE criterion expressed in these equations provides a more general method for calibrating the Hill (1950) model than the method of eqns (8). To illustrate: if the constant α in the Hill (1950) model are calibrated to fit the crystallographic yield surface computed by Bishop and Hill (1951a, b), one finds that

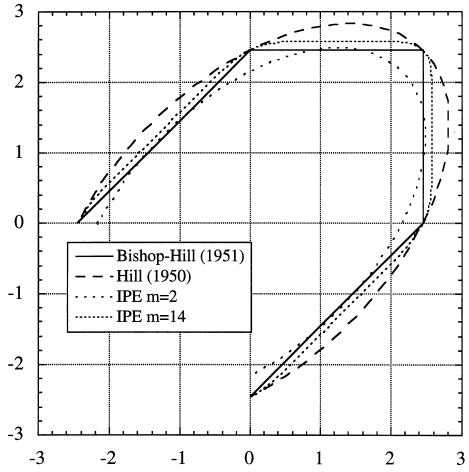

Fig. 2. Comparison of Hill (1950) and IPE $m = 2$ and $m = 14$ approximations to the Bishop and Hill (1951a, b) crystallographic fit. IPE fit parameters from Table 1.

$$\alpha_{12} = \alpha_{13} = \alpha_{23} = \frac{1}{6} Y^2 \left(\frac{1}{\tau_c^2}\right)$$

$$\alpha_{44} = \alpha_{55} = \alpha_{66} = \frac{1}{18} Y^2 \left(\frac{1}{\tau_c^2}\right), \tag{16}$$

where Y is the arbitrarily chosen 'equivalent' yield stress and τ_c is the critical resolved shear stress. Equations (8) calibrate the fit in eqn (16) based on a 'sample' of the crystal yield surface at six points. In contrast, the IPE equivalents of the Hill α's

$$\alpha_{12} = \alpha_{13} = \alpha_{23} = (a-c)^2,$$

$$\alpha_{44} = \alpha_{55} = \alpha_{66} = b^2, \tag{17}$$

are fit by the objective function to the crystal yield surface based on a sample of the surface at 80 points. The fit of eqns (8) has the Hill (1950) continuum yield surface circumscribe the Bishop and Hill (1951a, b) crystallographic surface, with intersections at each of the crystal surface vertices. The IPE-based fit is weighted more toward the crystal yield surface plane midpoints. Figure 2 displays a projection of both fits in the T_{11}–T_{12} plane, along with a projection of the crystal yield surface and a projection of a non-quadratic IPE yield surface. The quadratic IPE yield function exactly matches the Hill (1950) yield function (when both are calibrated to the Bishop and Hill (1951a, b) surface) when

$$(a-c) = 1.249239,$$

$$b = 0.721249. \tag{18}$$

2.3. Polycrystals

In general, each crystal (or grain) in a polycrystalline aggregate has an orientation associated with it which may be defined by a rotation tensor between the global reference frame and the

lattice reference frame. Let $\boldsymbol{L}^{\mathrm{c}}$ be the IPE transformation tensor for a single crystal with its lattice oriented to align with the natural lattice coordinates and with components as given in eqn (3). Let the number of grains in the polycrystal be denoted by N, and let $g = 1, \ldots, N$ denote the specific grains in the polycrystal. The linear IPE transformation tensor for each grain in the polycrystal with respect to a global orthonormal coordinate system can then be expressed in indicial notation as:

$$L^g_{ijkl} = R^g_{mi} R^g_{nj} R^g_{pk} R^g_{ql} L^{\mathrm{c}}_{mnpq}, \tag{19}$$

where $\boldsymbol{L}^g$ is the linear transformation tensor for grain g with respect to a fixed global reference frame and $\mathbf{R}^g$ is the rotation tensor from the global reference frame back to the lattice reference frame for grain g. As noted above, that the components of $\boldsymbol{L}^g$ have the symmetries $L^g_{ijkl} = L^g_{jikl} = L^g_{ijlk} = L^g_{klij}$.

The linear transformation tensor of a polycrystalline aggregate can be determined from that of each grain contained in the aggregate by averaging the effect of each grain. The question is then, what is the appropriate average to use? Karafillis and Boyce (1993) proposed that the work dissipation rate of the anisotropic material is equal to that of the IPE material. Therefore

$$\dot{W} = \mathbf{T} \cdot \mathbf{D}^{\mathrm{p}} = \mathbf{S} \cdot \mathbf{d}^{\mathrm{p}} = \boldsymbol{L}[\mathbf{T}] \cdot \mathbf{d}^{\mathrm{p}} \tag{20}$$

where $\dot{W}$ is the work dissipation rate due to plastic deformation, $\mathbf{D}^{\mathrm{p}}$ is the plastic rate of deformation tensor on the physical material, and $\mathbf{d}^{\mathrm{p}}$ is the plastic rate of deformation tensor on the IPE material. The dot ($\cdot$) denotes a tensor inner product defined as $\mathbf{T} \cdot \mathbf{D}^{\mathrm{p}} \equiv \mathrm{tr}(\mathbf{T}^{\mathrm{T}} \mathbf{D}^{\mathrm{p}})$ where superscript T denotes the transpose and tr( ) is the trace operator. Because the components of $\boldsymbol{L}$ have the major symmetries, $L_{ijkl} = L_{klij}$, eqn (20) can be rewritten as

$$\dot{W} = \mathbf{T} \cdot \mathbf{D}^{\mathrm{p}} = \mathbf{T} \cdot \boldsymbol{L}[\mathbf{d}^{\mathrm{p}}]. \tag{21}$$

For eqn (21) to be satisfied,

$$\mathbf{D}^{\mathrm{p}} = \boldsymbol{L}[\mathbf{d}^{\mathrm{p}}] + \boldsymbol{\Omega} \tag{22}$$

where $\boldsymbol{\Omega}$ is a symmetric, deviatoric, second-order tensor orthogonal to $\mathbf{T}$. Assuming associated flow, the rate of plastic deformation on the physical material, D^{p}_{ij}, is directed normal to the yield surface, expressed mathematically as

$$D^{\mathrm{p}}_{ij} = \dot{\lambda} \frac{\partial f}{\partial T_{ij}}, \quad f = |s_1 - s_2|^m + |s_2 - s_3|^m + |s_3 - s_1|^m - 2Y^m. \tag{23}$$

Applying the chain rule to eqn (23) and substituting eqn (2):

$$D^{\mathrm{p}}_{ij} = \dot{\lambda} \frac{\partial f}{\partial S_{kl}} \frac{\partial S_{kl}}{\partial T_{ij}} = d^{\mathrm{p}}_{kl} L_{klij}, \quad d^{\mathrm{p}}_{kl} = \dot{\lambda} \frac{\partial f}{\partial S_{kl}}, \tag{24}$$

where associated flow has been assumed in the IPE domain as well, as expressed by the second eqn in (24). Comparing (22) with (24), it can be seen that for normality to be satisfied in both the physical and IPE domain, $\boldsymbol{\Omega} = 0$; therefore,

$$\mathbf{D}^{\mathrm{p}} = \boldsymbol{L}[\mathbf{d}^{\mathrm{p}}]. \tag{25}$$

The relation between deformation rates given in eqn (25) is assumed to hold for both a single crystal and a polycrystalline aggregate.

If an aggregate is composed of N grains with various orientations, the linear transformation tensor of the aggregate can be derived by assuming that the work dissipation rates of the physical-domain polycrystal and corresponding IPE material are the same. In material micromechanics, the macroscale stress and deformation rate are taken to be equal to the volume averages of the microscale stresses and deformation rates. Also, it is standard to assume that the volume average of the product of the stress and deformation tensors over any representative volume element (RVE) is approximately equal to the product of their respective averages, i.e.:

$$\left(\frac{1}{N}\sum_{g=1}^{N} T^g \cdot D^g\right) \approx \left(\frac{1}{N}\sum_{g=1}^{N} T^g\right) \cdot \left(\frac{1}{N}\sum_{g=1}^{N} D^g\right). \tag{26a}$$

This assumption is strictly valid whenever (a) the rate of deformation in each grain is identical and is equal to the macroscale rate of deformation (Taylor, 1938 assumption); or when (b) the stress in each grain is identical and is equal to the macroscale stress (Sachs, 1928 assumption). Also, if the characteristic length of microscale features is suitably small, the assumption is valid as well (Nemat-Nasser and Hori, 1993). Using the assumption of eqn (26a), the global work dissipation rate for an aggregate $\dot{W}$ can be expressed as

$$\dot{W} = \left(\frac{1}{N}\sum_{g=1}^{N} \mathbf{T}^g\right) \cdot \left(\frac{1}{N}\sum_{g=1}^{N} \mathbf{D}^{\mathrm{p}g}\right) = \bar{\mathbf{T}} \cdot \bar{\mathbf{D}}^{\mathrm{p}}, \tag{26b}$$

where superscript g denotes the gth grain and an overbar ($^-$) indicates an arithmetic average. It should be noted that the averages defined in (26b) are volume averages if it is assumed that all of the grains have approximately the same volume.

Using Taylor's (1938) assumption that each grain within an aggregate undergoes the same deformation rate as the whole, eqn (26b) can be rewritten as

$$\dot{W} = \bar{\mathbf{T}} \cdot \mathbf{D}^{\mathrm{p}}, \tag{27}$$

where $\mathbf{D}^{\mathrm{p}} = \bar{\mathbf{D}}^{\mathrm{p}} = \mathbf{D}^{\mathrm{p}g}$ for $g = 1, \ldots, N$. In a similar way, the work dissipation rate can be expressed for an IPE material corresponding to an aggregate as

$$\dot{W} = \left(\frac{1}{N}\sum_{g=1}^{N} \mathbf{S}^g\right) \cdot \left(\frac{1}{N}\sum_{g=1}^{N} \mathbf{d}^{\mathrm{p}g}\right) = \bar{\mathbf{S}} \cdot \bar{\mathbf{d}}^{\mathrm{p}}, \tag{28}$$

where $\bar{\mathbf{S}}$ is the average (macroscopic) stress on the IPE material, and $\bar{\mathbf{d}}^{\mathrm{p}}$ is the average (macroscopic) rate of deformation tensor on the IPE material. Applying the relationship in eqn (25) to each grain in eqn (28), using Taylor's (1938) interaction law, making use of the symmetries of $\boldsymbol{L}^g$, and equating to (27):

$$\dot{W} = \bar{\mathbf{S}} \cdot \left(\frac{1}{N}\sum_{g=1}^{N} \boldsymbol{L}^{g^{-1}}[\mathbf{D}^{\mathrm{p}}]\right) = \bar{\mathbf{S}} \cdot \left(\frac{1}{N}\sum_{g=1}^{N} \boldsymbol{L}^{g^{-1}}\right)[\mathbf{D}^{\mathrm{p}}] = \bar{\mathbf{S}} \cdot \bar{\boldsymbol{L}}^{-1}[\mathbf{D}^{\mathrm{p}}] = \bar{\boldsymbol{L}}^{-1}[\bar{\mathbf{S}}] \cdot \mathbf{D}^{\mathrm{p}} = \bar{\mathbf{T}} \cdot \mathbf{D}^{\mathrm{p}},$$

(29)

where $\bar{\boldsymbol{L}}$ is taken to be the linear transformation tensor for the aggregate on the macroscale. So,

$$\bar{\boldsymbol{L}} = \left(\frac{1}{N} \sum_{g=1}^{N} \boldsymbol{L}^{g^{-1}} \right)^{-1} \tag{30}$$

is used to define the homogenized macroscopic linear transformation of the Cauchy stress to the IPE stress.

It is important to note that the homogenized form $\bar{\boldsymbol{L}}$ given by eqn (30) will meet the constraints of eqns (12) (which guarantee that yielding in the physical domain will be independent of the mean stress) as long as the form of $\boldsymbol{L}^{\mathrm{c}}$ used in the computations meets these constraints. Consider first that the transformation $\boldsymbol{L}^{g}$, computed by eqn (19), will meet these constraints. If $\mathbf{T}'$ is deviatoric, then, in global coordinates, $\mathbf{S}$ will be given by

$$S_{ij} = L^{g}_{ijmn} T'_{mn} = R^{g}_{pi} R^{g}_{qj} R^{g}_{rm} R^{g}_{sn} L^{\mathrm{c}}_{pqrs} T'_{mn}, \tag{31a}$$

or in direct notation

$$\mathbf{S} = \mathbf{R}^{g^{\mathrm{T}}} (\boldsymbol{L}^{\mathrm{c}} [\mathbf{R}^{g} \mathbf{T}' \mathbf{R}^{g^{\mathrm{T}}}]) \mathbf{R}^{g} \Rightarrow \mathbf{R}^{g} \mathbf{S} \mathbf{R}^{g^{\mathrm{T}}} = \boldsymbol{L}^{\mathrm{c}} [\mathbf{R}^{g} \mathbf{T}' \mathbf{R}^{g^{\mathrm{T}}}]. \tag{31b}$$

The right-hand side of the second form in (31b) is deviatoric,

$$\mathrm{tr}(\mathbf{R}^{g} \mathbf{T}' \mathbf{R}^{g^{\mathrm{T}}}) = \mathrm{tr}(\mathbf{R}^{g^{\mathrm{T}}} \mathbf{R}^{g} \mathbf{T}') = \mathrm{tr}(\mathbf{T}') = 0, \tag{32a}$$

so $\mathbf{S}$ is also deviatoric,

$$\mathrm{tr}(\mathbf{R}^{g} \mathbf{S} \mathbf{R}^{g^{\mathrm{T}}}) = \mathrm{tr}(\mathbf{R}^{g^{\mathrm{T}}} \mathbf{R}^{g} \mathbf{S}) = \mathrm{tr}(\mathbf{S}) = 0, \tag{32b}$$

and thus $\boldsymbol{L}^{g}$ and $\boldsymbol{L}^{g^{-1}}$ meet the constraint:

$$\mathbf{S}' = \boldsymbol{L}^{g}[\mathbf{T}'], \quad \boldsymbol{L}^{g^{-1}}[\mathbf{S}'] = \mathbf{T}'. \tag{33}$$

Now, if it is assumed that the macroscale IPE stress $\bar{\mathbf{S}}'$ is deviatoric, the relationship between $\bar{\mathbf{S}}'$ and $\bar{\mathbf{T}}$, the macroscale physical stress, is

$$\left(\frac{1}{N} \sum_{g=1}^{N} \boldsymbol{L}^{g^{-1}} \right) [\bar{\mathbf{S}}'] = \left(\frac{1}{N} \sum_{g=1}^{N} \boldsymbol{L}^{g^{-1}} [\bar{\mathbf{S}}'] \right) = \bar{\mathbf{T}}. \tag{34}$$

Rearranging (34), it is apparent that each term on the left-hand side is deviatoric:

$$\mathrm{tr} \left(\sum_{g=1}^{N} \boldsymbol{L}^{g^{-1}} [\bar{\mathbf{S}}'] \right) = \sum_{g=1}^{N} \mathrm{tr}(\boldsymbol{L}^{g^{-1}} [\bar{\mathbf{S}}']) = N \, \mathrm{tr}(\bar{\mathbf{T}}) = 0, \tag{35}$$

so $\bar{\mathbf{T}}$ is also deviatoric, and $\bar{\boldsymbol{L}}$ meets the constraint

$$\bar{\mathbf{S}}' = \bar{\boldsymbol{L}}[\bar{\mathbf{T}}']. \tag{36}$$

If the yielding in individual crystals of a polycrystal is pressure-independent, the yielding of the polycrystalline aggregate must also be pressure-independent. Equation (36) shows that the homogenization scheme of eqn (30) preserves on the macroscale the pressure-independent yielding

of the microscale, as would be necessary for the homogenization scheme to be legitimate. Because eqn (36) holds, the IPE yield criterion may be used as a generalization of Hill's (1950) criterion not only for single crystals (as discussed in Section 2.2), but also for polycrystalline aggregates.

3. *R*-values

The *R*-value is defined as the ratio of the transverse plastic strain increment to the thickness strain increment during a uniaxial tensile test. Usually, the tensile tests will be performed at different angles with respect to the rolling direction in the plane of a sheet and the *R*-value will be reported as a function of the angle. This parameter is commonly used to indicate the degree of anisotropy in rolled sheet metals.

Recall that under the assumption of associated flow, the IPE transformation tensor $\boldsymbol{L}$ relates not only the physical and IPE stresses, but also the physical and IPE plastic rates of deformation, as was shown in eqn (25):

$$\mathbf{D}^{\mathrm{p}} = \boldsymbol{L}[\mathbf{d}^{\mathrm{p}}]. \tag{25}$$

Underlying this equation was the assumption of associated flow in both the IPE domain and the physical domain. Assuming associated flow on both the grain level and homogenized macroscopic level, eqn (25) applies to both the grains and the overall polycrystal.

The procedure for determining *R*-values follows immediately from this relation. For a given macroscopic stress, $\bar{\mathbf{T}}$, use the linear transformation tensor in eqn (30) to determine the macroscopic IPE stress $\bar{\mathbf{S}}$. Then using the relations in eqn (24) along with the yield function in (4), determine the components of the rate of deformation tensor in terms of $\dot{\lambda}$. Letting the increment of plastic strain be approximated by $\mathrm{d}\varepsilon^{\mathrm{p}}_{ij} \approx \mathbf{D}^{\mathrm{p}}_{ij}\,\mathrm{d}t$, then the *R*-value can be expressed as the ratio

$$R = \frac{\mathrm{d}\varepsilon^{\mathrm{p}}_{22}}{\mathrm{d}\varepsilon^{\mathrm{p}}_{33}} \approx \frac{D^{\mathrm{p}}_{22}}{D^{\mathrm{p}}_{33}}, \tag{37}$$

where the 1-, 2- and 3-axes represent the tensile direction, the transverse direction and the thickness direction, respectively.

4. Numerical examples

The IPE method developed above is first used to compute the yield surfaces of fcc polycrystals for some commonly observed textures. These textures include the brass, copper and S textures (each with 50% random texture) which result from moderate deformation processes, and the cube and goss textures (also with 50% random texture) which form after recrystallization processes. Table 2 gives the Miller indices of the ideal orientations for these special textures. These textures are generated by assuming that the grain orientations are rotationally symmetric Gaussian distributions about the ideal orientation of each texture, which can be expressed as

$$g(\omega) = g(0)\exp\left(-\frac{\omega^2}{2\omega_0^2}\right). \tag{38}$$

Table 2
Miller indices of the ideal orientations of several special textures

Texture	Miller indices
Brass	$\{110\}\langle 1\bar{1}2\rangle$
Copper	$\{112\}\langle 11\bar{1}\rangle$
S	$\{123\}\langle 63\bar{4}\rangle$
Cube	$\{100\}\langle 001\rangle$
Goss	$\{110\}\langle 001\rangle$

In eqn (38), $g(0)$ is the density of the ideal orientation, ω_0 represents the scatter width of the spread and $g(\omega)$ is the relative density of a given orientation rotated through an angle ω from the ideal orientation.

In order to maintain orthotropic symmetry, four equivalent ideal orientations, i.e. $(hkl)[uvw]$, $(\bar{h}\bar{k}\bar{l})[uvw]$, $(hkl)[\bar{u}\bar{v}\bar{w}]$ and $(\bar{h}\bar{k}\bar{l})[\bar{u}\bar{v}\bar{w}]$, are used in creating the grain orientation distributions. Following the procedure adopted by Lequeu et al. (1987a), the orientations of each grain are created according to eqn (38) with $\omega_0 = 5^\circ$. Figures 3(a)–(f) show the $\{111\}$ pole figures of these special textures and the random texture, each figure constructed of 400 grains. In these figures, RD means the following direction of the sheet and TD is the transverse direction in the plane of the sheet.

The uniaxial yield strength of the random texture is first calculated using the IPE method with different exponents m in the yield function eqn (4). For the isotropic aggregate that results from a random texture, Bishop and Hill (1951a, b) and Viana et al. (1979) have used crystallographic considerations to calculate a relation between the critical resolved shear stress of a single crystal and the macroscopic yield stress Y of the polycrystal. The relationship for an fcc crystal/polycrystal was found to be

$$Y = 3.06\tau_c. \tag{39}$$

Compared with the IPE method outlined above, the IPE prediction of yield stress is more or less constant and identical to $3.06\tau_c$ over a range of exponents $m = 3$ to $m = 10$. The yield strength corresponding to $m = 6$ is exactly $3.06\tau_c$, and the value deviates from this by no more than $0.2\tau_c$ when m is not close to 6, but is between $3 \leqslant m \leqslant 10$. Because the deviation from the Bishop–Hill result is greatest at lower values of m, in the following examples, only those m values which are in the range $4 \leqslant m \leqslant 10$ will be considered.

Barlat and Richmond (1987) use the Bishop and Hill (1951a, b) model (with the Taylor, 1938 interaction law) to construct yield surfaces for a number of textures that are 50% special/50% random. Pole figures of the random and special textures used are shown in Figs 3(a)–(f). The IPE method developed in this paper is used to calculate the yield surfaces of these same textures. With the IPE method, the yield surfaces can be constructed using all six stress components. However, to simplify the problem, only a plane stress condition is considered. Figure 4 shows the yield

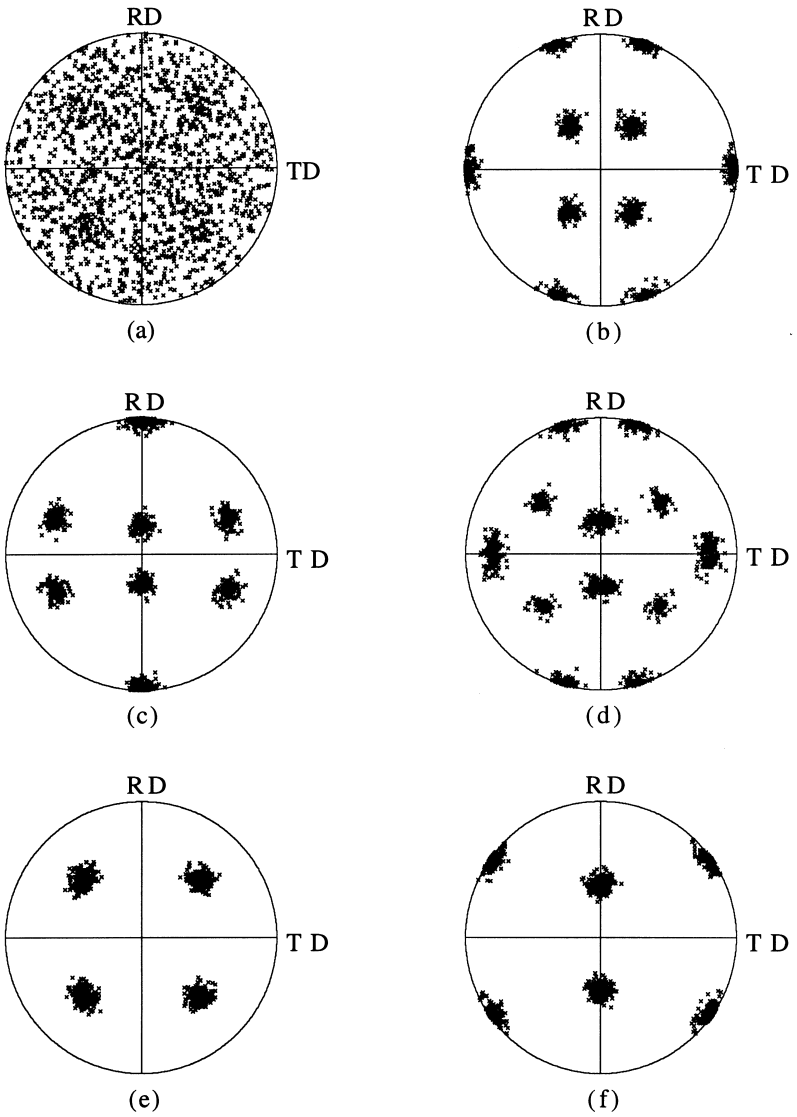

Fig. 3. {111} pole figure of different textures modeled with 400 grains by assuming rotationally symmetric Gaussian distribution with $\omega_0 = 5^\circ$. (a) Random, (b) brass, (c) copper, (d) S, (e) cube, (f) goss.

surfaces for a random texture computed for four different values of m, i.e., $m = 4$, 6, 8 and 10. The parameter s represents the ratio of shear stress to the yield strength for uniaxial tension in the rolling direction, i.e. $s = \bar{T}_{12}/Y$. The yield surfaces corresponding to different shear stress ratios s are calculated, and the projections of these yield surfaces on the normalized $\bar{T}_{11}$–$\bar{T}_{22}$ plane are plotted. The yield surfaces constructed by larger m have flatter bounding planes. This is expected, since the yield function used, eqn (4), becomes the straight-sided Tresca criterion when m approaches infinity. Figure 5 plots the yield surfaces of the 50% brass/50% random texture, which

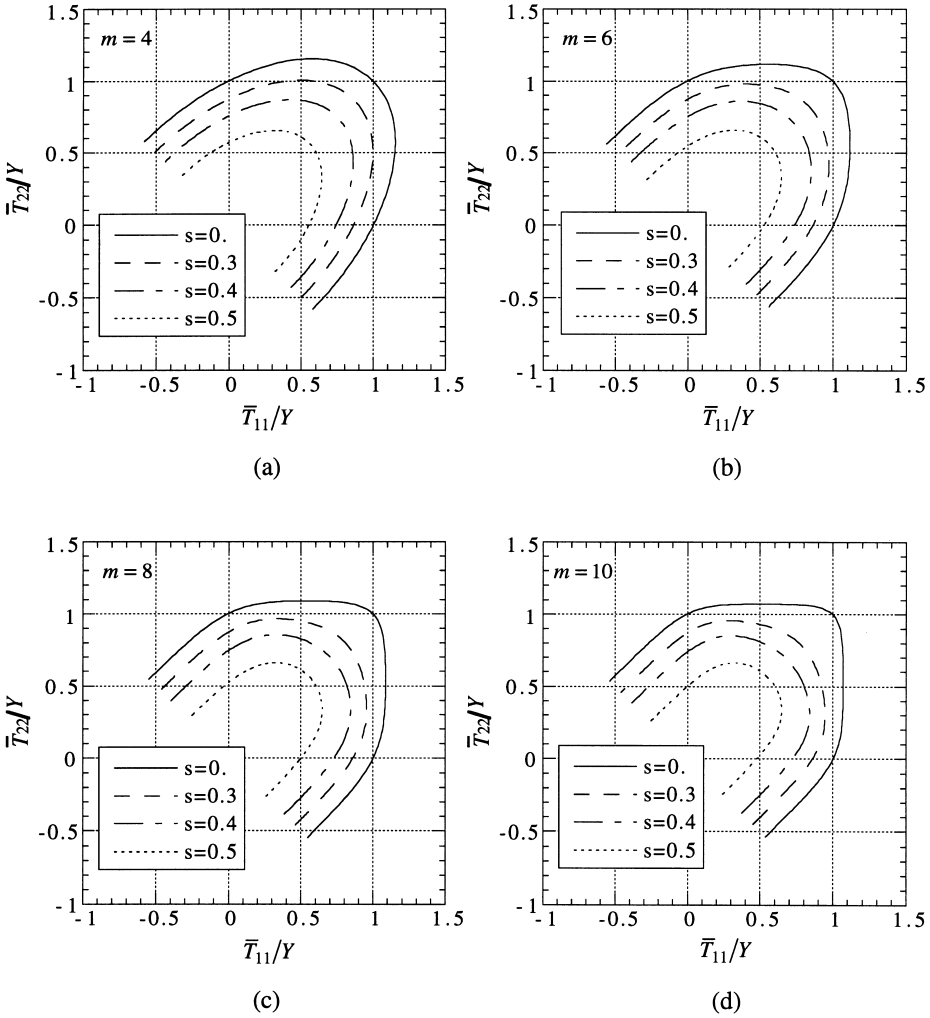

Fig. 4. Yield surfaces for a random texture with different shear stress effect, where $s = \bar{T}_{12}/Y$. Different values of exponent m are used: (a) $m = 4$; (b) $m = 6$; (c) $m = 8$; (d) $m = 10$.

show a larger yield stress in the transverse direction ($\bar{T}_{22}$) than in the rolling direction ($\bar{T}_{11}$). Notice that in Figs 5(c) and (d), the yield surfaces corresponding to $s = 0.5$ do not exist. The ratio $s = 0.5$ is larger than the critical resolved shear stress ratio and so $s = 0.5$ corresponds to points on the yield surface where $\bar{T}_{11} = T_{22} = 0$. In general, as larger values of m are used in the governing IPE yield functions, the magnitude of s that plots to the $\bar{T}_{11}$–$\bar{T}_{22}$ plane decreases. The yield surfaces for the 50% copper/50% random texture, shown in Fig. 6, have larger yield stresses in the rolling direction than in the transverse direction, in direct contrast to the yield surfaces the 50% brass/50% random texture. Figure 7 shows the yield surfaces of the 50% S/50% random texture, which is similar to that of a random texture when $s = 0$. When the shear stress effect is considered, the random and 50% S/50% random surfaces are quite different. Figures 8 and 9 show the yield

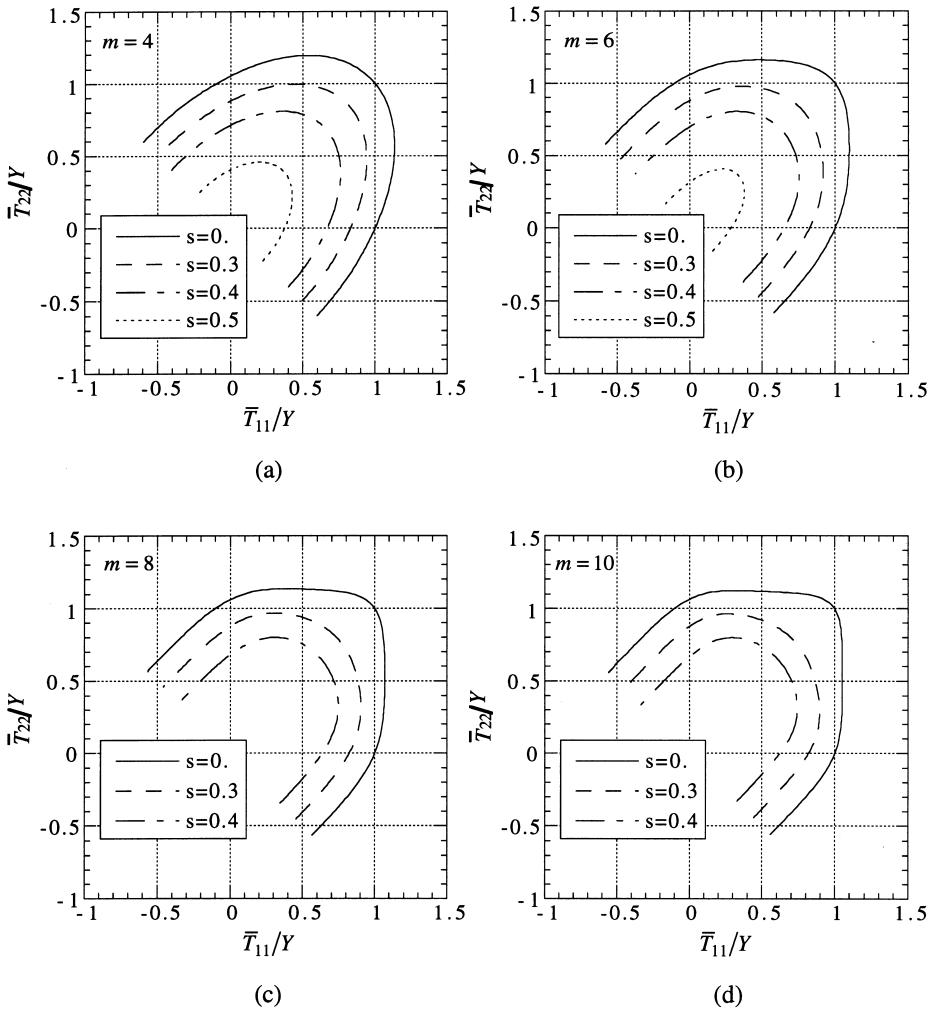

Fig. 5. Yield surfaces for a texture including 50% brass texture and 50% random texture. Different values of exponent m are used: (a) $m = 4$; (b) $m = 6$; (c) $m = 8$; (d) $m = 10$.

surfaces for the 50% cube/50% random and 50% goss/50% random textures. The 50% goss/50% random texture exhibits strong anisotropy in the sheet plane, with a significantly larger yield stress in the transverse direction than in the rolling direction. The yield surfaces for the 50% cube/50% random texture are similar to those of the purely random texture. This similarity stems from the fact that the cube texture has cubic properties which are symmetric with respect to both the rolling direction and the transverse direction (see Fig. 3(e)), and thus the yield surfaces are symmetric about the line $\bar{T}_{11} = \bar{T}_{22}$.

Comparing Figs 4–9 with the results of Barlat and Richmond (1987), who use the Bishop and Hill (1951a, b) crystallographic method, it is apparent that the Barlat and Richmond (1987) yield surfaces have flatter sides, similar to those computed by the IPE method with $m = 8$. Considering

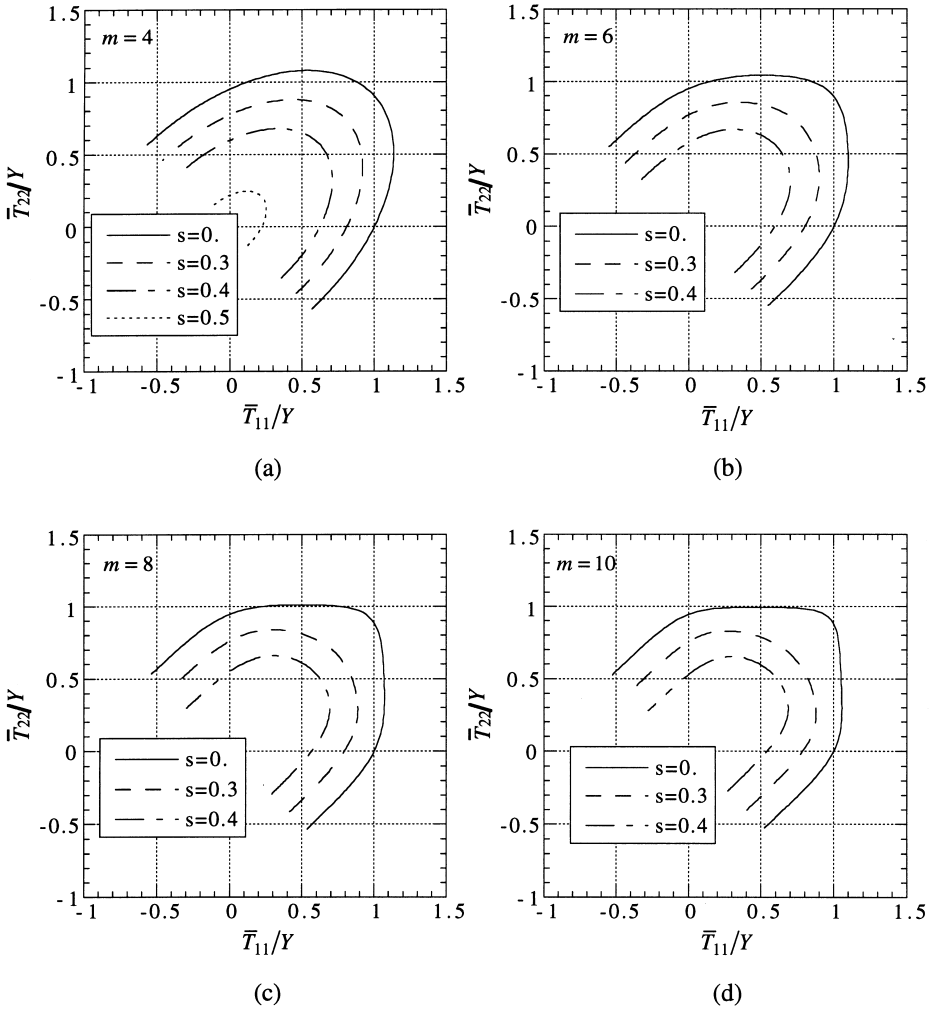

Fig. 6. Yield surface for a texture including 50% copper texture and 50% random texture. Different values of exponent m are used: (a) $m = 4$; (b) $m = 6$; (c) $m = 8$; (d) $m = 10$.

that the yield surface of a single fcc crystal is composed of planes, it is expected that the yield surfaces derived by a purely crystallographic approach like that of Bishop and Hill (1951a, b) will be flat-sided. In the IPE method, because the yielding of a single fcc crystal is modeled by eqn (4), the computed surface may be either flat or curved, depending on the exponent m chosen.

The degree of anisotropy of a textured polycrystal is difficult to evaluate from the yield surface; R-values are generally used to serve this purpose. To illustrate the effect of texture on the R-value, R-values for various textures are calculated as a function of θ, the angle between the uniaxial tensile direction and the rolling direction. Figures 10(a)–(e) show the R-value distributions for the textures with yield surfaces displayed in Figs 5–9. For the 50% brass/50% random texture, the highest R-value is found around $\theta = 50^\circ$, with $R \approx 1$ at $\theta = 90^\circ$ and $R < 1$ at $\theta = 0^\circ$. The highest

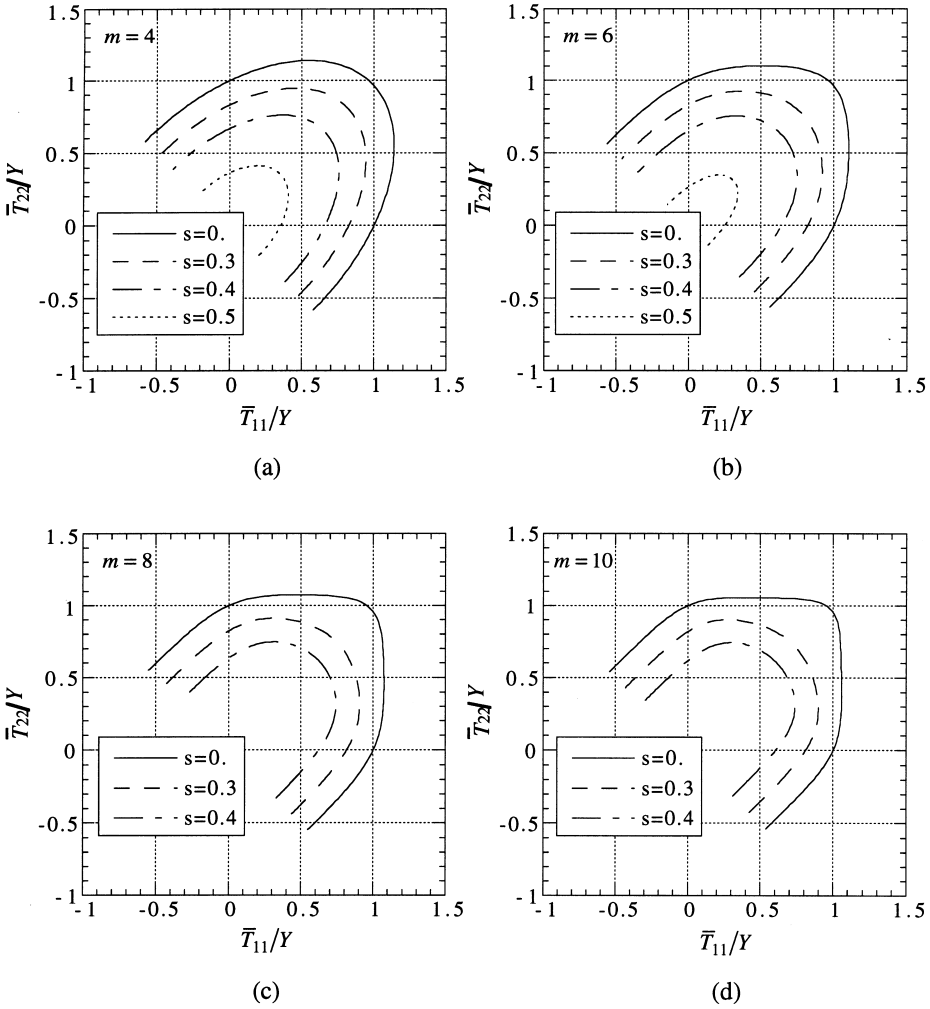

Fig. 7. Yield surfaces for a texture including 50% S texture and 50% random texture. Different values of exponent m are used: (a) $m = 4$; (b) $m = 6$; (c) $m = 8$; (d) $m = 10$.

R-value for the 50% copper/50% random texture appears near $\theta = 40^\circ$, with $R \approx 1$ at $\theta = 0^\circ$ and $R < 1$ at $\theta = 90^\circ$. It is interesting to note that the R-value distribution of the 50% copper/50% random texture is just like the distribution of the 50% brass/50% random texture reflected about $\theta = 45^\circ$. (This symmetry is similar to that seen in the yield surfaces of these two textures.) The R-value distribution for the 50% S/50% random texture is nearly symmetric about $\theta = 45^\circ$, with the highest value at $\theta = 45^\circ$ and the lowest value at $\theta = 0^\circ$ and $\theta = 90^\circ$. For the 50% cube/50% random texture, the R-value distribution is also symmetric about $\theta = 45^\circ$, but with the lowest R-value at $\theta = 45^\circ$ and the highest R-value, $R = 1$, at $\theta = 0^\circ$ and $\theta = 90^\circ$. The R-value of the 50% goss/50% random texture is very high at $\theta = 90^\circ$; it decays from its peak at $\theta = 90^\circ$ to a minimum near $\theta = 40^\circ$, then increases slightly from $\theta = 40^\circ$ to $\theta = 0^\circ$. At $\theta = 0^\circ$, for the 50% goss/50%

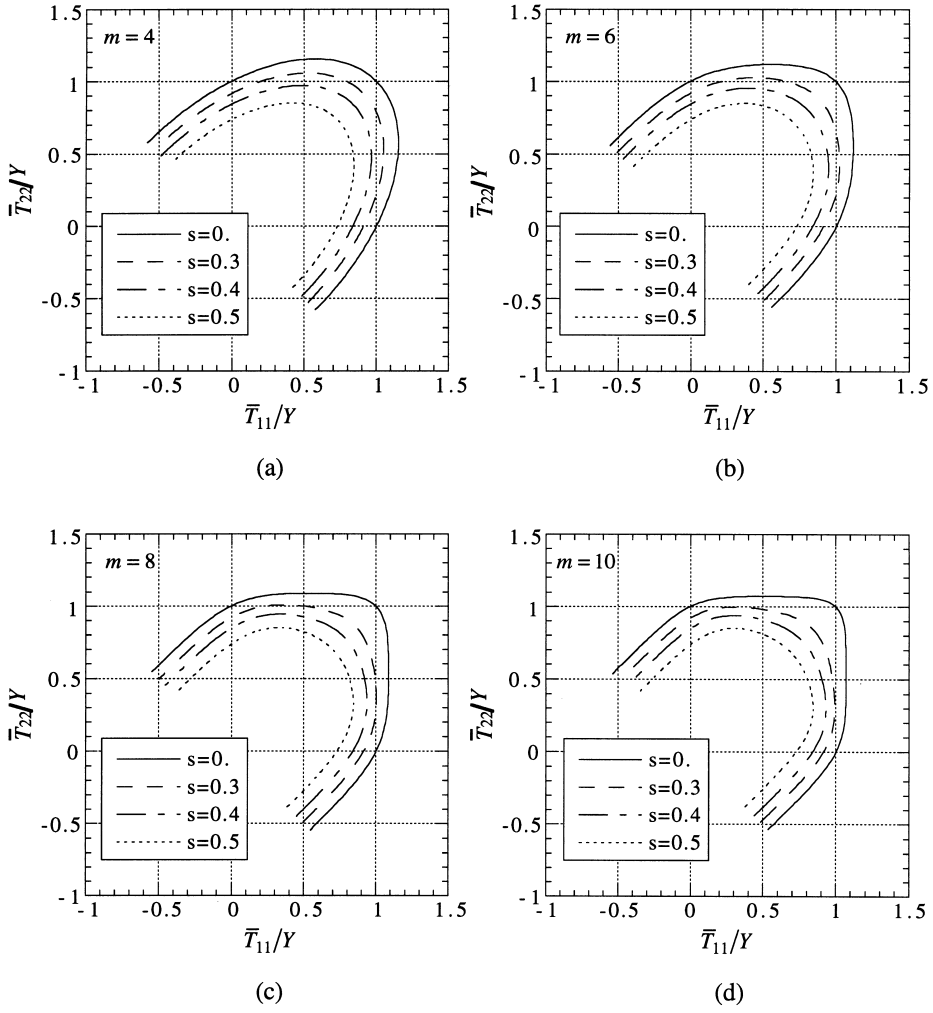

Fig. 8. Yield surfaces for a texture including 50% cube texture and 50% random texture. Different values of exponent m are used: (a) $m = 4$; (b) $m = 6$; (c) $m = 8$; (d) $m = 10$.

random texture $R = 1$. The R-value distributions calculated by the IPE method are quite similar to those obtained by Lequeu et al. (1987a, b) who used a continuum function to model the plastic behavior of polycrystalline metals. Figure 11 compares experimentally determined R-values for a 2008-T4 aluminum with the R-values computed by the IPE method. As the figure shows, the IPE R-values correspond qualitatively with those found in experiments.

5. Conclusion

A continuum anisotropic yield criterion for textured metal polycrystals is developed by using a homogenization scheme to link the continuum IPE method of Karafillis and Boyce (1993) to the

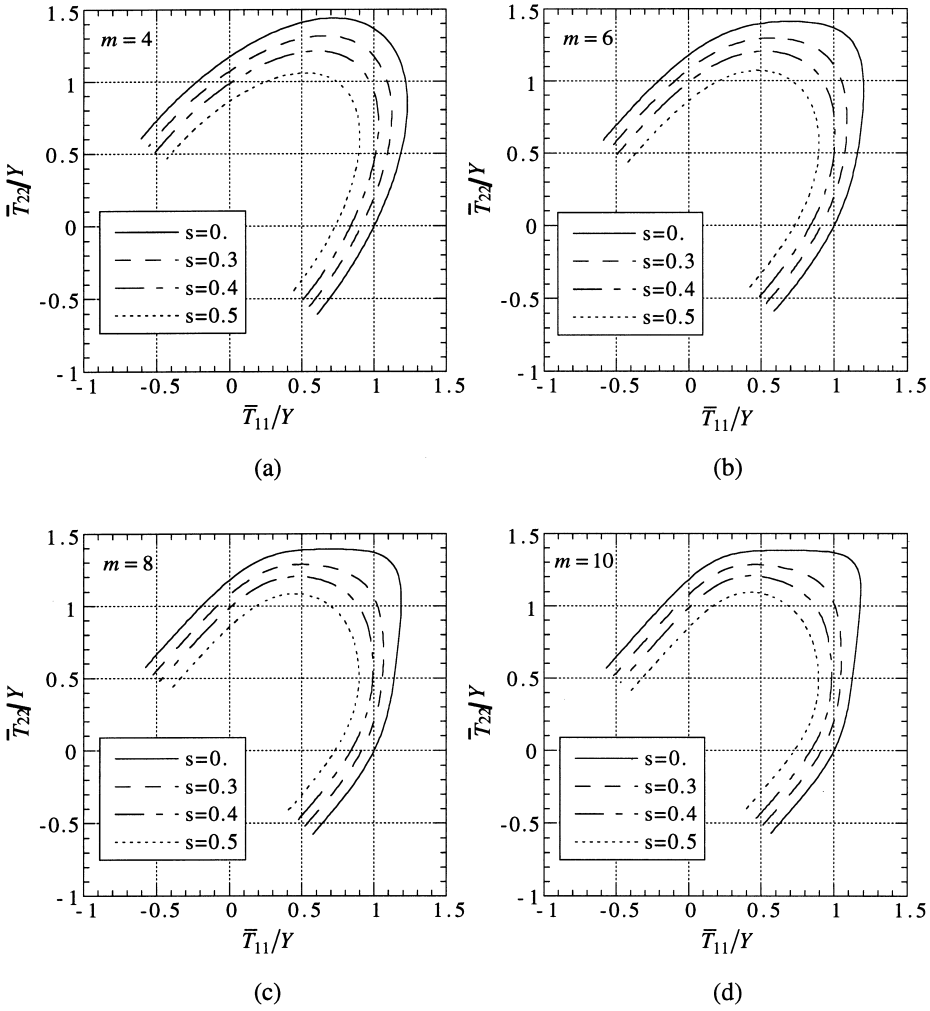

Fig. 9. Yield surfaces for a texture including 50% goss texture and 50% random texture. Different values of exponent m are used: (a) $m = 4$; (b) $m = 6$; (c) $m = 8$; (d) $m = 10$.

crystallographic method of Bishop and Hill (1951a, b). The homogenization scheme developed produces a continuum yield function for a polycrystal that accounts for the effect of polycrystalline texture on yielding behavior, and that also preserves on the macroscale the pressure-independent yielding behavior observed on single crystals on the microscale. This new IPE criterion can be viewed as a generalization of the Hill (1950) anisotropic criterion, adding to Hill's criterion the ability to describe non-quadratic yielding behavior, the ability to account for microstructural texture, and the ability to choose the number of data points used to calibrate the model. Yield surfaces and R-values predicted by this method correspond well with the yield surfaces and R-values predicted by more cumbersome crystallographic methods, and the R-value predictions correspond reasonably well with experimental data. The method proves to obtain some of the

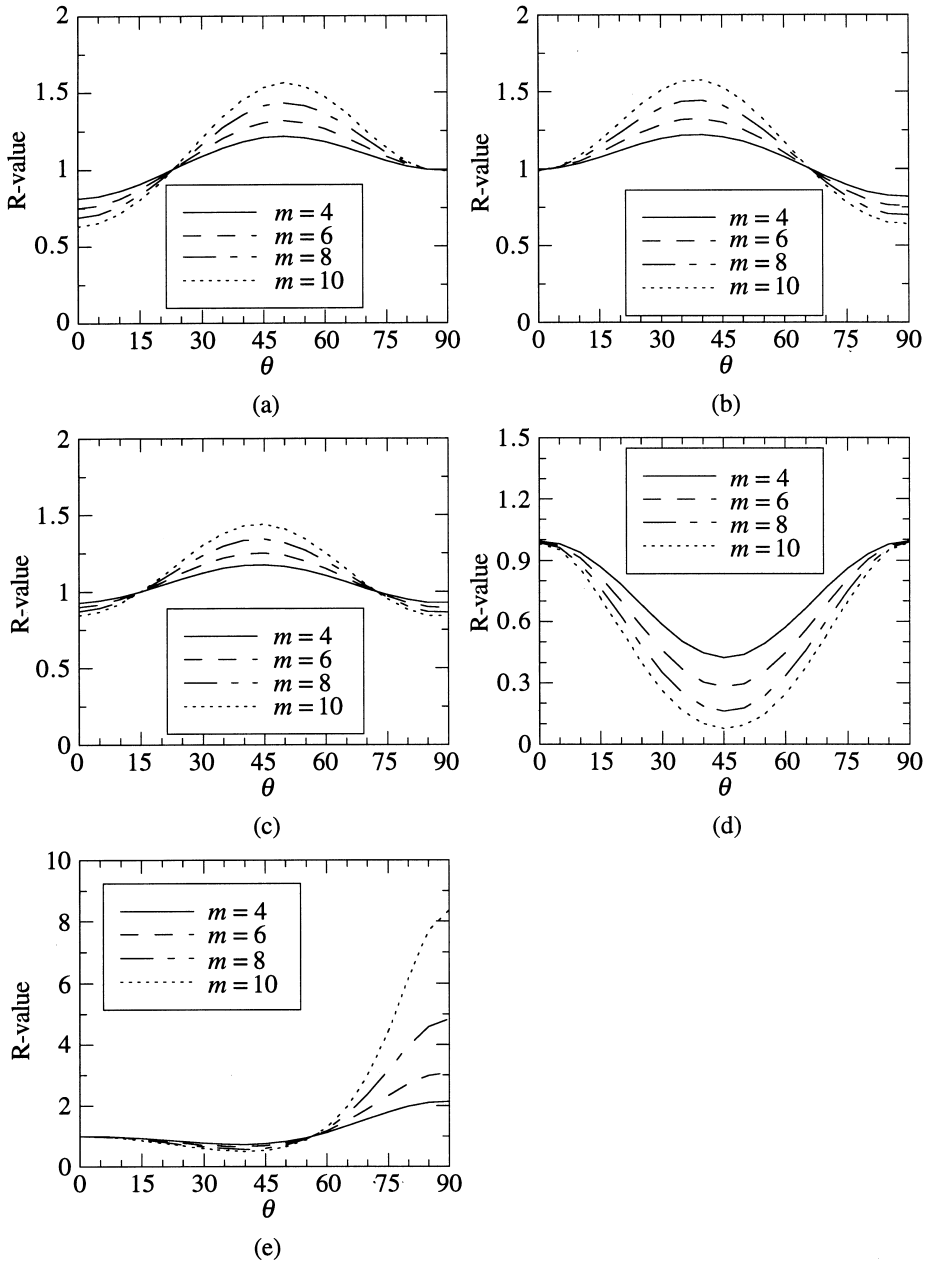

Fig. 10. *R*-value distributions for the following textures: (a) brass; (b) copper; (c) S; (d) cube; (e) goss.

accuracy of crystallographic methods, while preserving the computational efficiency of other, less accurate phenomenological methods.

The model is particularly well-suited for implementation into design packages based on the finite element method. Expected improvements in the homogenization method and the development of

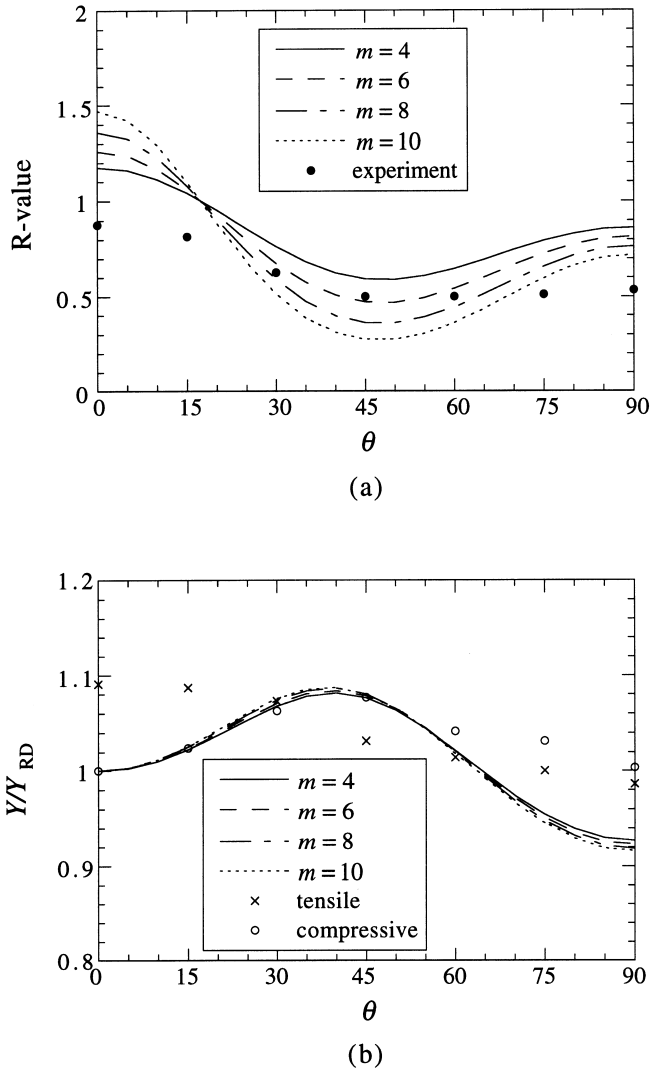

Fig. 11. Material anisotropy predicted by the IPE method and compared with experimental data for 2008-T4 sheet. (a) *R*-value, (b) yield strengths.

evolution rules promise to give the method broad applicability in aiding the design with textured polycrystalline metals.

Acknowledgements

This work was supported by the Henry Luce Foundation, Inc. and by the National Science Foundation through Grant DMI-9358123.

References

Barlat, F., Richmond, O., 1987. Prediction of tricomponent plane stress yield surface and associated flow and failure behavior of strongly textured F.C.C. polycrystalline sheets. Mater. Sci. Eng. 95, 15–29.

Barlat, F., Lege, D.J., Brem, J.C., 1991. A six-component yield function for anisotropic materials. Int. J. Plasticity 7, 693–712.

Barlat, F., Maeda, Y., Chung, K., Yanagawa, M., Brem, J.C., Hayashida, Y., Lege, D.J., Matsui, K., Murtha, S.J., Hattori, S., Becker, R.C., Makosey, S., 1997. Yield function development for aluminum alloy sheets. J. Mech. Phys. Solids 45, 1727–1763.

Bishop, J.F.W., Hill, R., 1951a. A theory of the plastic distortion of a polycrystalline aggregate under combined stresses. Phil. Mag. 42, 414–427.

Bishop, J.F.W., Hill, R., 1951b. A theoretical derivation of the plastic properties of a polycrystalline face-centered metal. Phil. Mag. 42, 1298–1307.

Gurtin, M.E., 1981. An Introduction to Continuum Mechanics. Academic Press, New York.

Harren, S.V., 1991. The finite deformation of rate dependent polycrystals—I. A self-consistent framework. J. Mech. Phys. Solids 39, 345–360.

Hill, R., 1950. The Mathematical Theory of Plasticity. Clarendon Press, Oxford.

Hill, R., 1965. Continuum micro-mechanics of elastoplastic polycrystals. J. Mech. Phys. Solids 13, 89–101.

Hosford, W.F., 1972. A generalized isotropic yield criterion. J. Appl. Mech. 39, 607–609.

Karafillis, A.P., Boyce, M.C., 1993. A general anisotropic yield criterion using bounds and a transformation weighting tensor. J. Mech. Phys. Solids 41, 1859–1886.

Kocks, U.F., Canova, G.R., Jonas, J.J., 1983. Yield vectors in FCC crystals. Acta Metall. 31, 1243–1252.

Lequeu, P.H., Gilormini, P., Montheillet, F., Bacroix, B. and Jonas, J.J., 1987a. Yield surfaces for textured polycrystals—I: Crystallographic approach. Acta Metall. 35, 439–451.

Lequeu, P.H., Gilormini, P., Montheillet, F., Bacroix, B., Jonas, J.J., 1987b. Yield surfaces for textured polycrystals—II: Analytic approach. Acta Metall. 35, 1159–1174.

Lian, J., Barlat, F., Baudelet, B., 1989. Plastic behaviour and stretchability of sheet metals. Part II: Effect of yield surface shape on sheet forming limit. Int. J. Plasticity 5, 131–147.

Nemat-Nasser, S., Hori, M., 1993. Micromechanics: Overall Properties of Heterogeneous Materials, Section 2.6. North-Holland, Amsterdam.

Nye, J.F., 1957. Physical Properties of Crystals; Their Representation by Tensors and Matrices. Oxford University Press, London.

Sachs, G., 1928. Zur Ableitung einer Fliessbedingung (on the derivation of a yield condition). Ver. Dtsch. Ing. 72, 734–736.

Taylor, G.I., 1938. Plastic strains in metals. J. Inst. Metals 62, 307–324.

Taylor, G.I., Elam, C.F., 1925. The plastic extension and fracture of aluminum crystals. Proc. Roy. Soc. A 108, 28–51.

Viana, C.S., Da, C., Kallend, J.S., Davies, G.J., 1979. The use of texture data to predict the yield locus of metal sheets. Int. J. Mech. Sci. 21, 355–371.